information

MDPI

Article

User Pairing and Power Allocation for NOMA-CoMP Based on Rate Prediction

Jiang Wu , Leyang Sun and Yubo Jia *

Department of Information and Communication Engineering, Zhejiang Sci-Tech University, Hangzhou 310018, China; wujiang@zstu.edu.cn (J.W.); 201920601007@mails.zstu.edu.cn (L.S.)
* Correspondence: jiayubo1964@zstu.edu.cn

Abstract: In this paper, we consider a non-orthogonal multiple access (NOMA) system with coordinated multi-point (CoMP), which is used in 5G cellular networks to guarantee the rate requirements from the different edge users. Based on the China Family Panel Studies (CFPS) dataset, we use several learning algorithms to predict users' rate requirements according to their profiles. We propose a many-to-many two-side subchannel–user matching strategy, which can classify users into cell-center users, high-rate requirement edge users, and low-rate requirement edge users based on their status and learning prediction results, and pair users with different subchannels to form joint transmission CoMP (JT-CoMP) subchannels and dynamic point selection CoMP (DPS-CoMP) subchannels. Furthermore, a discrete power allocation algorithm based on group search is proposed. Simulation results show that our proposed algorithm outperforms the traditional NOMA-CoMP algorithm and maximum throughput (MT) NOMA-CoMP algorithm. It maximizes the rate of high-rate requirement edge users while guaranteeing user fairness.

Keywords: non-orthogonal multiple access (NOMA); coordinated multi-point (CoMP); users classification and subchannel scheduling; discrete power allocation

check for updates

Citation: Wu, J.; Sun, L.; Jia, Y. User Pairing and Power Allocation for NOMA-CoMP Based on Rate Prediction. *Information* **2022**, *13*, 200. https://doi.org/10.3390/info13040200

Academic Editor: Lorenzo Mucchi

Received: 1 March 2022
Accepted: 13 April 2022
Published: 15 April 2022

1. Introduction

In 5G and beyond 5G (B5G) wireless cellular networks, non-orthogonal multiple access(NOMA) has great potential in improving spectrum efficiency and network throughput [1–3]. Coordinated multi-point (CoMP) is applied to the scenario of multiple cells, which can reduce the interference between cells, and improve the system throughput at the same time [4–6]. The interferences arisen in different sectors of the same cell or different cells can be aligned or mitigated by CoMP technologies. The traditional orthogonal frequency division multiplexing (OFDM)-CoMP system can reduce inter-cell interference (ICI) and increase the transmission rate of cell-edge users, but each subchannel can only schedule one user in each time slot. Due to the deployment of 5G dense cellular networks, NOMA systems need to solve problems such as improving the efficiency of cell resource scheduling and reducing ICI. Therefore, it is an important research work to study NOMA resource scheduling based on CoMP. In addition, the performance of 5G wireless networks is greatly affected by efficient user clustering and scheduling, power allocation, and CoMP transmission mode. In order to further improve the performance of the NOMA-CoMP network system, it is necessary to establish a network model with differentiated user rates and use a matching theory for user classification and optimization algorithms for power allocation.

1.1. Existing Research

The basic idea of NOMA is to use non-orthogonal transmission at the transmitting end, introduce interference information actively, and achieve correct demodulation through a serial interference cancellation (SIC) receiver at the receiving end. Spectrum efficiency can be significantly improved by allowing multiple users to share the same subchannel in the power domain. Therefore, it is widely studied and applied to 5G access technology [7–10]. Wireless network joint resource allocation and scheduling significantly impact system spectrum efficiency and network throughput [11,12]. In [13], considering a downlink NOMA network, the authors studied power allocation issues while scheduling subchannels, and a subchannel–user matching algorithm was proposed by exploiting the many-to-many two-side matching theory. The results proved that the algorithm was better than orthogonal frequency division multiple access (OFDMA) schemes. Based on [13], a new algorithm was proposed to solve a two-side exchange stable matching problem, and its results showed that the proposed algorithm outperforms traditional OMA and NOMA schemes [14]. A proportional fairness scheduling scheme for NOMA to maximize normalized rate was studied in [15].

Edge users are usually far away from base stations (BSs). With NOMA technology alone, edge users may not meet their quality of service (QoS) requirements. To solve this problem, CoMP transmission was used in [16,17] to improve the throughput of edge users. Recently, resource scheduling for NOMA-CoMP networks has attracted a lot of attention. In downlink CoMP networks, an opportunistic NOMA (ONAMA) system was proposed in [18,19]. It was shown that the performance of an ONOMA-CoMP system is better than traditional joint transmission (JT) NOMA-CoMP. In [20], a multi-tier NOMA (TNOMA) scheme was proposed for CoMP networks to increase a high-transmission-rate service range. In [21,22], different clustering scenarios were investigated, where the authors discussed a beamforming scheme in downlink NOMA systems and considered power allocation. Various network scenarios with different user spatial distributions and derivation of a user achievable rate expression in different NOMA-CoMP scenarios were discussed in [23,24]. In [25], the authors proposed a power optimization method that maximizes energy efficiency in downlink NOMA-CoMP networks. However, the subchannel allocation and power allocation issues are not well discussed in the existing works. JT-NOMA and Alamouti-NOMA (A-NOMA) are proposed in [26] to reduce the outage probabilities in a simultaneous wireless information and power transfer (SWIPT) network. The result shows that A-NOMA performs better than both JT-NOMA and JT-OMA in high SNR. In [27], a metaheuristic teaching–learning-based optimization (TLBO) algorithm is proposed to optimize the energy efficiency in a hybrid satellite-unmanned aerial vehicle (UAV) relay network (HSURN) based on the downlink NOMA transmission and CoMP. There are two NOMA clustering models in [28] in order to improve user sum-rate and reduce user SIC complexity. One is Unlimited NOMA clustering (UNC) where the order of each NOMA cluster is the maximum possible value. Another is limited NOMA clustering (LNC) where the SIC is performed for only a subset of users to improve user sum-rate and reduce user SIC complexity. JT-CoMP is applied with full-duplex (FD) cooperative NOMA (C-NOMA) to maximize the network sum-rate while guaranteeing the required quality-of-service of users [29].

A few works considered a joint subchannel and multi-cell power allocation problem in a NOMA-CoMP system. In [30], a multi-criteria user coordination mode selection algorithm based on coordinated NOMA was proposed. Two resource allocation algorithms were proposed considering the effects of imperfect channel state information (CSI) and SIC. Simulation results showed that the proposed method can effectively reduce energy consumption and improve user robustness. In [31], a maximum throughput (MT) algorithm for subchannel allocation for a NOMA-CoMP system was proposed, and its results showed that MT algorithm enhanced spectral efficiency. However, the authors assumed an ideal condition without any difference among subchannels of each cell, and performed user power allocation before subchannel allocation. A BS clustering algorithm based on successive convex approximation is proposed to improve system sum-rate and spectrum efficiency [32]. The simulation results show that the proposed scheme can increase the sum-rate even in high user density. Inspired by [13,31], we consider the case of subchannel differentiation in each CoMP cell and propose a many-to-many two-side matching strategy, where the subchannel allocation is performed prior to power allocation.

In order to introduce CoMP technology, we make a more specific analysis of CoMP types so as to establish a theoretical foundation for the following discussion. CoMP technology has three main scheduling modes, namely joint transmission (JT) [33], dynamic point selection (DPS) [34], and coordinated scheduling/coordinated beamforming (CS/CB) [35]. (1) In the JT mode, the BSs of different coordinated cells can perform joint scheduling to the same edge user on the same resource block (RB). The coordinated BSs can not only share the CSI of each subchannel and the user's scheduling information, but also exchange user data. Users can obtain power allocation and data transmission from BSs in the same time slot. This model can effectively convert ICI into desired signals and improve the overall cell throughput. However, scheduling information and data exchange between multiple BSs also brings high backhaul bandwidth and latency issues. (2) In the DPS mode, only one of the coordinated BSs in the cluster can be selected for scheduling edge users in the same time slot. According to the channel conditions between BSs and users, the system can dynamically select different BSs in different time slots to obtain the optimal data transmission. (3) In the CS/CB mode, the BSs of the coordinated cells share CSI and beamforming information, which can reduce or even eliminate ICI suffered by edge users. However, the coordinated BSs only schedule edge users in their respective cells and do not exchange user data. This greatly reduces the backhaul bandwidth overhead. In this paper, the types of downlink CoMP we use are JT mode and DPS mode. JT-CoMP has better coverage performance and stability, which can provide better performance gains. That is the reason why high rate requirement user is served by JT-CoMP. Moreover, DPS-CoMP has lower algorithm complexity, lower cost of returning to the city and lower system performance. So we use DPS-CoMP to serve low rate requirement users.

The rapid development of deep learning is better satisfying the stringent requirements of future cellular networks. Ref. [36] proposed a CoMP transmission method based on deep learning, which can immediately determine whether to use synchronous transmission or time-division multiplexing during the training process based on offline computer simulation. Ref. [37] studied user-centric networks and proposed a reinforcement learning (RL) framework based on neural fitting Q iterative technology, which can dynamically adjust the transmission and reception points involved in joint transmission. In [38], a method based on adaptive online learning was designed considering the inter-cell interference, which can perform dynamic clustering and carrier aggregation in the CoMP system to improve the throughput of the system. Refs. [39,40] adressed mobile network caching (MNC). Ref. [39] used community-aware non-negative matrix factorization (CNMF) with implicit feedback to predict the probability of content requests, and designed a CNMF-based active caching algorithm to estimate content requests by considering associated users and neighbor users in close collaboration with CoMP probability to make caching decisions. Ref. [40] proposed an online learning algorithm based on reinforcement learning to search for the best caching strategy considering practical time-varying user request patterns. Our work uses a deep learning algorithm to predict the user rate to ensure that edge users can be divided into high-rate requirement users and low-rate requirement users based on their mobile phone usage habits.

1.2. Motivation and Contributions

For most current NOMA-CoMP systems, there are some problems existing: (1) Most of the works assume that there is a significant difference in channel gain between users, so that users are paired according to channel quality. However, when the users are close to each other, their CSI is not much different, and the users cannot be distinguished and successfully paired in terms of channel gain, so that the advantages of NOMA-CoMP cannot be fully utilized; (2) in the future 5G actual network, the rate requirements from the edge users are not guaranteed to be fully achieved due to the low data rate at the edge areas and the high frequency handoff for edge users between cells in 5G networks [41,42].

Thus, it is very important to predict users' behaviors, especially their rate requirements before we implement the downlink CoMP among the edge users; (3) most of the work does not distinguish the required rate of users, which leads to the system applying many resources to edge users with low rate requirements according to the principle of the NOMA system, resulting in a waste of power resources. Therefore, it is very important to study the scenarios of using CoMP and NOMA for user rate differentiation and subchannel differentiation. This motivated our work.

In this paper, considering subchannel differentiation and user rate differentiation, we aim to maximize the rate of edge users with high-speed demand while ensuring user fairness. Our goal is to optimize joint subchannel scheduling and multi-cell power allocation. The main contributions of this work are summarized as follows.

- We implement a variety of machine learning algorithms based on real datasets to predict the rate requirements of edge users. This ensures that edge users can be classified into high-rate requirement edge users and low-rate requirement edge users.
- A many-to-many two-side subchannel user matching algorithm (MSUMA) for NOMA-CoMP systems is proposed to divide the subchannels into JT-CoMP subchannels and DPS-CoMP subchannels according to different scheduling users.
- For the power allocation, we propose a discrete power allocation algorithm based on group search. The performance of the proposed algorithm is evaluated and compared to the MT scheme and traditional NOMA-CoMP algorithm. Simulation results demonstrate that the proposed scheme outperforms the other schemes.

1.3. Paper Organization

The rest of the paper is organized as follows. Section 2 presents the NOMA-CoMP system model. In Section 3, we propose a learning method to predict the rate of user rate requirement and then build a model for predicting the rate of user rate requirement. Section 4 proposes a many-to-many two-side subchannel user matching algorithm for NOMA-CoMP systems. A discrete power allocation algorithm based on group search in NOMA-CoMP systems is proposed in Section 5, including power allocation algorithms in DPS-CoMP subchannels, JT-CoMP subchannels and between subchannels. Section 6 carries on the simulations to the above-mentioned algorithms. Finally, Section 7 summarizes the results and gives the conclusions of this paper.

2. System Model

A downlink multi-cell NOMA-CoMP wireless network is described in Figure 1. For simplicity of discussion, we only consider establishing a three-cell NOMA-CoMP network model. The analysis and simulation results under the model are applicable to the situation of more cells, as the formulas and the algorithms we proposed are based on the discussion of B cells, where the conclusion we draw is not effected by the number of cells.

There are 3 CoMP clusters in Figure 1 (i.e., one JT-NOMA-CoMP cluster and two DPS-NOMA-CoMP clusters). In the JT-NOMA-CoMP cluster, $UE^{C}_{B1,1}$ and $UE^{C}_{B2,1}$ are the cell-center users served by BS_1 and BS_2, respectively. $UE^{E}_{B1B2,1}$ is the high-rate requirement edge user from the prediction of the user behavior, which is expected to get the best service. Meanwhile, $UE^{E}_{B2,1}$ and $UE^{E}_{B3,1}$ are the low-rate requirement users from the user behavior prediction, which means they only need to be served with their target rate. In the *ts* time slot, $UE^{E}_{B2,1}$ and $UE^{E}_{B3,1}$ form NOMA-CoMP clusters with $UE^{C}_{B2,2}$ and $UE^{C}_{B3,1}$ through DPS-CoMP mode, respectively. According to the principle of NOMA, the subchannels of each cell are superimposed on multiple users for simultaneous transmission. Therefore, interference will occur on this subchannel, which is called intra-cell interference. In order to obtain the signal desired by the user accurately, the receiving end of each user adopts the SIC and the user can eliminate the intra-cell interference caused by other users whose channel gain is smaller than its own channel gain on the subchannel.

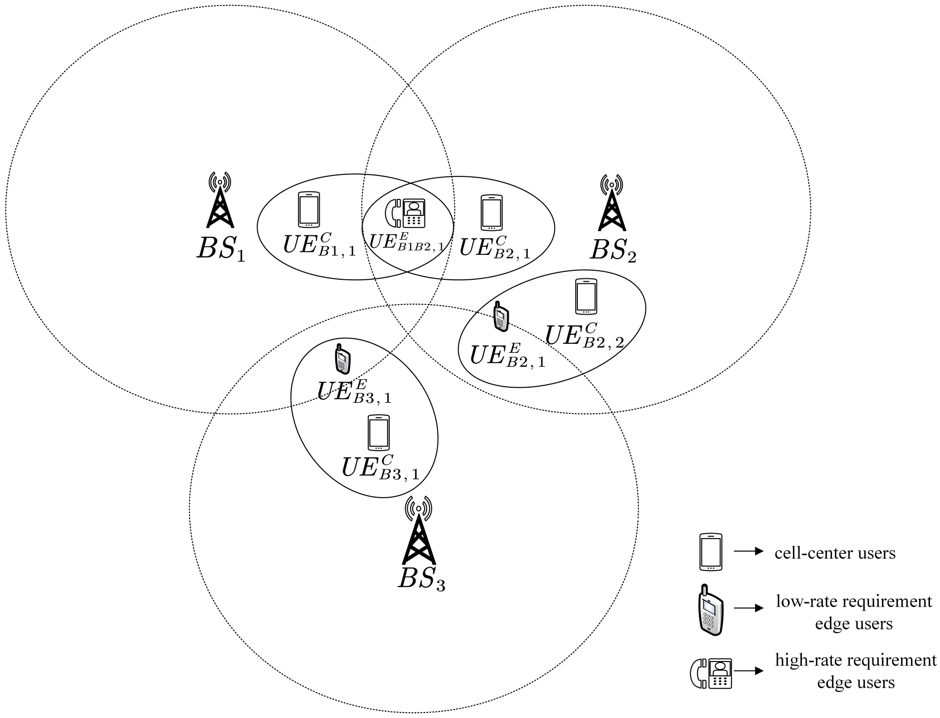

Figure 1. A system model of NOMA-CoMP networks.

First, we consider the DPS-NOMA-CoMP cluster. Each CoMP user is only scheduled by one CoMP-BS, and other CoMP-BSs will not cause interference to the user (i.e., there is no ICI). Consider a group of users $\boldsymbol{M} = \{1, ..., M\}$, where each user has a distinct channel gain. Moreover, suppose the SIC decoding order is based on the user's index, i.e., the signal of UE_1 is decoded first, then the signal of UE_2, and so on. Therefore, according to the SIC, UE_1 can decode its desired signal by treating the signals of all other users in the system as intra-cell interference. In this way, UE_m can decode its desired signal after eliminating all users whose channel gain is smaller than its own by applying SIC technology. In this DPS-NOMA-CoMP system, the achievable rate of any user l on subchannel k can be written as

$$R_{k,l} = \log_2\left(1 + \frac{x_{k,l}p_{k,l}\gamma_{k,l}}{\sum\limits_{l'=l+1}^{m} x_{k,l'}p_{k,l'}\gamma_{k,l} + \omega_l}\right) \quad (1)$$

where the channel is assumed to be a Rayleigh fading channel over bandwidth $B = 1$. $\gamma_{k,l}$ denotes the channel power gain for user l at the receiver, and $p_{k,l}$ represents the transmit power of user l. $x_{k,l}$ represents the channel selection parameter. When the subchannel k is allocated to the user l, the value is 1, otherwise it is 0. $\omega_l \sim \mathbb{C}N\left(0, \sigma_l^2\right)$ denotes additive white Gaussian noise (AWGN) at user l and σ_l^2 is the variance of the noise.

Then we consider the JT-NOMA-CoMP cluster. We assume that the users in this cluster are scheduled by at most two CoMP-BSs, denoted by BS_α and BS_β, respectively. The number of cell-center users in the cell α and β is defined as $\varphi_{c,\alpha}$ and $\varphi_{c,\beta}$, respectively, and the number of of edge users with high rate requirement is defined as φ_e. In this two-BS CoMP-set, the set of non-CoMP-UEs $i \in \{1, 2, \ldots, \varphi_{c,\alpha}\}$ in the cell α, the set of non-CoMP-UEs $j \in \left\{1, 2, \ldots, \varphi_{c,\beta}\right\}$ in the cell β , and the set of CoMP-UEs $e \in \{1, 2, \ldots, \varphi_e\}$ all are assumed to follow the SIC ordering according to their subscripts. Hence, the achievable data rate for the CCU i served by BS_α for $B = 1$ can be expressed as (in order to make the formula clear, we omit the part where the channel selection parameter $x_{k,i}$ is 0):

$$R_i = \log_2\left(1 + \frac{p_i^\alpha \gamma_i^\alpha}{\sum_{i'=i+1}^{\varphi_{c,\alpha}} p_{i'}^\alpha \gamma_i^\alpha + \left|\left|\mathbf{p}_j^\beta\right|\right|_1 \gamma_i^\beta + \omega_i}\right) \tag{2}$$

where γ_i^α and γ_i^β denote the CCU i's channel gain with BS_α (desired channel) and with BS_β(ICI channel), respectively. p_i^α represents the transmit power of the CCU i from BS_α, while $\sum_{i'=i+1}^{\varphi_{c,\alpha}} p_{i'}^\alpha$ represents the power of other cell-center users from BS_α who are matched into the same JT-CoMP subchannel with the user i but have higher SIC ordering. $\left|\left|\mathbf{p}_j^\beta\right|\right|_1 = \sum_{j=1}^{\varphi_{c,\beta}} p_j^\beta$ represents the transmit power of cell-center users from BS_β, which form the NOMA-CoMP cluster at BS_β end with the same edge users (i.e., the transmit power of ICI).

The achievable data rate for the CCU j served by BS_β can be expressed as

$$R_j = \log_2\left(1 + \frac{p_j^\beta \gamma_j^\beta}{\sum_{j'=j+1}^{\varphi_{c,\beta}} p_{j'}^\beta \gamma_j^\beta + \left|\left|\mathbf{p}_j^\alpha\right|\right|_1 \gamma_i^\alpha + \omega_j}\right) \tag{3}$$

where γ_j^β and γ_j^α represent the CCU j's channel gain with BS_β (desired channel) and with BS_α (ICI channel), respectively. The terms p_j^β and $\sum_{j'=j+1}^{\varphi_{c,\beta}} p_{j'}^\beta$ are similar to Equation (2) but in terms of CCU j in the cell β. As well, $\left|\left|\mathbf{p}_i^\alpha\right|\right|_1 = \sum_{i=1}^{\varphi_{c,\alpha}} p_i^\alpha$ denotes the power for cell-center users from BS_α which form the NOMA-CoMP cluster at BS_α end with the same edge users.

The achievable data rate for the edge user e, from the same JT-NOMA-CoMP cluster as in Equations (2) and (3), can be expressed as

$$R_e = \log_2\left(1 + \frac{\boldsymbol{P}_e^T \gamma_e}{I_e + \omega_e}\right) \tag{4}$$

where

$$I_e = \sum_{e'=e+1}^{\varphi_e} \boldsymbol{P}_{e'}^T \gamma_e + \sum_{i=1}^{\varphi_{c,\alpha}} p_i^\alpha \gamma_e^\alpha + \sum_{j=1}^{\varphi_{c,\beta}} p_j^\beta \gamma_e^\beta \tag{5}$$

The term $\boldsymbol{P}_e^T \gamma_e = p_e^\alpha \gamma_e^\alpha + p_e^\beta \gamma_e^\beta$ denotes the desired signal transmitted from both CoMP-BSs (BS_α and BS_β), where $\boldsymbol{P}_e = \left[p_e^\alpha, p_e^\beta\right]^T$, $\gamma_e = \left[\gamma_e^\alpha, \gamma_e^\beta\right]^T$ and $\boldsymbol{P}_e^T$ indicates the transpose of $\boldsymbol{P}_e$. $\sum_{e'=e+1}^{\varphi_e} \boldsymbol{P}_{e'}^T \gamma_e$ represents intra-cell interference caused by other users in the cluster who have higher SIC ordering. $\sum_{i=1}^{\varphi_{c,\alpha}} p_i^\alpha \gamma_e^\alpha$ and $\sum_{j=1}^{\varphi_{c,\beta}} p_j^\beta \gamma_e^\beta$ are the ICI from two jointly scheduled CoMP-BSs, BS_α and BS_β, respectively.

In this system model, we need to maximize the sum data rate of CoMP users in the JT-NOMA-CoMP cluster, while ensuring that the CoMP users in the DPS-NOMA-CoMP cluster and the non-CoMP users in the two clusters reach their target rate. P_k and P_{total} represent the power budget on the k-th subchannel and the total system power budget. We assume that the number of users multiplexed on each subchannel is M. The range of M is $M_f \leq M \leq M_u$, where M_u is the upper bound of the multiplexed user on the subchannel and M_f is the lower bound. The optimization problem is expressed as

$$\max_{x_{k,n},p_{k,n}} \sum_{k\in \boldsymbol{K}} \sum_{n\in \boldsymbol{e}} R_{k,n} \tag{6}$$

$$s.t.\ C1: \sum_{n\in \boldsymbol{N}} p_{k,n} \leq P_k \tag{7}$$

$$C2: \sum_{k\in \boldsymbol{K}} \sum_{n\in \boldsymbol{N}} p_{k,n} \leq P_{total} \tag{8}$$

$$C3: R_i \geq R_i^{\min}, \forall i = 1, \ldots, \varphi_{c,\alpha} \tag{9}$$

$$C4: R_j \geq R_j^{\min}, \forall j = 1, \ldots, \varphi_{c,\beta} \tag{10}$$

$$C5: R_e \geq R_e^{\min}, \forall k = 1, \ldots, \varphi_e \tag{11}$$

$$C6: R_l \geq R_l^{\min}, \forall l = 1, \ldots, \varphi_l \tag{12}$$

$$C7: x_{k,n} \in \{0,1\} \quad \forall k \in \boldsymbol{K}, \quad n \in \boldsymbol{N} \tag{13}$$

$$C8: M_f \leq \sum_{n\in \boldsymbol{N}} x_{k,n} \leq M_u \tag{14}$$

Since the transmission power of the BS and the power allocation of each subchannel is limited, the power allocation variable $p_{k,n}$ must meet the constraints C1, C2. Constraints C3–C6, respectively, represent the the minimum rate requirement of non-CoMP user i served by BS_α, and non-CoMP user j served by BS_β, CoMP user e jointly scheduled by BS_α and BS_β, and user l in the DPS-NOMA-CoMP cluster. Constraint C7 indicates whether a discrete binary variable $x_{k,n}$ is allocated. Constraint C8 ensures that each subchannel can only be allocated at most M_u users.

Due to the structure of the optimization function and the existence of discrete variables $x_{k,n}$ and continuous variables $p_{k,n}$, the entire optimization problem has the characteristics of mixed integer nonlinear programming (MINLP), whose optimal solution is difficult to determine. However, in practical systems, the power is typically set in discrete steps. In this way, we discretize the entire optimization problem to facilitate our following work. We predict the requirement rate of users in Section 3 to ensure that edge users can be divided into two varieties.

3. Predict and Leverage Users' Rate Requirements

In this section, we predict the user requirement rate based on the China Family Panel Studies (CFPS) dataset. Assuming that the base station can obtain user information completely, we can classify the edge users into high-rate requirement and low-rate requirement by the user's predicted rate.

3.1. Introduction of Machine Learning Algorithms

Random forest is to construct a forest in a random way, and there are many decision trees in the forest. In random forests, there is no relationship between each decision tree. After getting the forest, let each decision tree in the forest make a judgment separately when a new input sample comes in. Determine which category the sample should belong to, and then determine which category is selected the most, and predict which category the sample belongs to.

The linear discriminant analysis algorithm tries to find a line so that the projections of points of the same class on the line are as close as possible, and the projections of points of different classes on the line are as far as possible. When a new sample point needs to be classified, the projection of the point on the straight line is calculated, and the classification of the new sample point is judged according to the projection position.

Naive Bayes classification is a method based on Bayes' theorem and assuming that the feature conditions are independent of each other. First, learn the joint probability distribution from input to output through the given training set, with the assumption that the feature words are independent. Then, based on the learned model, input X to find the output that maximizes the posterior probability of Y.

Support vector machine (SVM) is a binary classification model whose basic model is a linear classifier that defines the largest margin in the feature space. SVMs also include kernel tricks, which make them essentially non-linear classifiers. The learning strategy of SVM is interval maximization, which can be formalized as a problem of solving convex quadratic programming, The learning algorithm of SVM is an optimization algorithm for solving convex quadratic programming.

K-Nearest Neighbor (KNN) is one of the simplest machine learning algorithms that can be used for classification and regression, and it is a supervised learning algorithm. Its main idea is that if most of the K nearest neighbors of a sample in the feature space belong to a certain class, then the sample also belongs to that class and has the characteristics of the samples in that class. The KNN method only determines the class of samples to be classified based on the class of one or more recent samples.

RUS refers to random undersampling, which randomly selects a certain amount of majority class samples and minority class samples from the dataset to form a training dataset with a balanced distribution. Boost refers to the Adaboost algorithm, which means that the algorithm adds RUS technology to the Adaboost algorithm. The Adaboost algorithm is an ensemble learning algorithm. Its core idea is to train different classifiers (weak classifiers) for the same training set, and then combine these weak classifiers to form a stronger final classifier (strong classifier). The RUSBoost algorithm changes the random sampling of the Adaboost algorithm to the sampling technology of unbalanced data, which greatly improves the accuracy of the classification of unbalanced data sets.

3.2. User Requirement Rate Prediction

We use the latest data released by CFPS and select 17,498 samples about mobile phones (other samples have nothing to do with mobile phone use or refuse to answer questions related to mobile phone using habits). Using the users' profiles as features, we predict the user's communication habits as labels. These characteristics are all independent variables that may affect the user's communication habits which are the user's profile. For the data released by CFPS, we screen out about 45 features from 1371 variables.

In order to predict the rate requirements of users through features, we use "the frequency of using the Internet to entertain" and "the frequency of using the Internet to contact" to express the rate requirements of video services and the rate requirements of text services (e.g., WeChat or email), respectively. According to the dataset's quality, two labels are selected to represent the user's requirement rate: (1) The frequency of using the Internet to entertain and (2) the frequency of using the Internet to contact. Correspondingly, each label is represented by five levels (inaccurate frequency) in CFPS: (1) Almost every day, (2) several times a week, (3) several times a month, (4) sometimes, (5) never or do not answer. Specifically, "almost every day" is denoted by 1, and "never or do not answer" is denoted by 5.

Next, we use machine learning methods to predict the user's communication habits. Specifically, we use random forest, linear discriminant, naive Bayes, linear support vector machine (SVM), and k-nearest neighbor (KNN). In addition, we also design a learning method based on the RUSBoost algorithm to predict the communication habits of users. RUSBoost is an algorithm for dealing with class imbalance problems in data with discrete class labels. It uses a combination of RUS (random undersampling) and the standard boosting program AdaBoost to model the minority classes better.

We provide confusion matrices for predicting the "frequency of using the Internet to entertain" and "the frequency of using the Internet to contact" in Figures 2 and 3 to evaluate the performance of different learning algorithms, respectively. We use digitd with color in Figures 2 and 3 for correct predictions. During simulation, we use cross-validation to prevent overfitting by dividing the dataset into 10 groups and estimating the accuracy of each group. The row shows the number of users with the real value, and the column shows the prediction number of users.

Predicted\Real	1	2	3	4	5
1	6649	1784	42	1	0
2	2612	3137	126	9	1
3	400	747	87	6	0
4	53	172	22	5	0
5	0	1	0	0	1641

Tree

Predicted\Real	1	2	3	4	5
1	6749	1636	44	2	0
2	2692	3092	96	4	1
3	338	813	85	4	0
4	41	171	36	4	0
5	0	1	0	0	1642

Linear Discriminant

Predicted\Real	1	2	3	4	5
1	6110	2330	29	2	5
2	2675	3159	48	0	3
3	401	815	23	1	0
4	71	173	5	1	2
5	0	1375	0	1	266

Native Bayes

Predicted\Real	1	2	3	4	5
1	7053	1416	3	4	0
2	2801	3065	14	4	1
3	427	808	3	2	0
4	59	188	2	3	0
5	0	1	0	0	1641

SVM

Predicted\Real	1	2	3	4	5
1	5207	2782	420	66	1
2	2750	2573	473	86	3
3	514	552	139	34	1
4	89	118	39	6	0
5	27	26	7	1	1581

KNN

Predicted\Real	1	2	3	4	5
1	5860	2782	399	884	0
2	1816	2573	625	1539	1
3	214	552	271	513	0
4	25	118	45	149	0
5	0	0	0	0	1642

RUSBoosted Trees

Predicted\Real	1	2	3	4	5
1	8476	0	0	0	0
2	0	5885	0	0	0
3	0	0	1240	0	0
4	0	0	0	252	0
5	0	0	0	0	1642

100% Accuracy

Predicted\Real	1	2	3	4	5
1	6225	975	395	851	0
2	1241	3066	643	934	1
3	162	111	640	327	0
4	30	28	36	158	0
5	0	0	0	0	1642

Learning Method based on the Rusboost Algorithm

Figure 2. Confusion matrix for predicting the frequency of using the Internet to entertain.

Predicted\Real	1	2	3	4	5
1	9633	1203	5	16	1
2	2279	1811	1	22	1
3	253	288	0	9	0
4	185	239	1	12	0
5	1	0	0	0	1535

Tree

Predicted\Real	1	2	3	4	5
1	9857	980	0	20	1
2	2501	1566	0	46	0
3	244	279	0	27	0
4	160	234	0	43	0
5	0	1	0	0	1536

Linear Discriminant

Predicted\Real	1	2	3	4	5
1	6386	4455	4	2	11
2	1155	2947	6	5	0
3	144	404	0	2	0
4	112	321	1	3	0
5	616	0	0	0	920

Native Bayes

Predicted\Real	1	2	3	4	5
1	10141	707	6	3	1
2	2639	1465	3	6	0
3	281	262	3	4	0
4	202	230	2	3	0
5	1	0	0	0	1535

SVM

Predicted\Real	1	2	3	4	5
1	8087	2411	218	139	4
2	2259	1560	184	107	3
3	264	225	25	33	3
4	197	182	34	24	0
5	20	22	2	1	1491

KNN

Predicted\Real	1	2	3	4	5
1	7731	1859	415	852	1
2	1103	1649	399	962	0
3	104	143	130	173	0
4	76	80	79	202	0
5	0	0	0	0	1536

RUSBoosted Trees

Predicted\Real	1	2	3	4	5
1	10858	0	0	0	0
2	0	4114	0	0	0
3	0	0	551	0	0
4	0	0	0	438	0
5	0	0	0	0	1537

100% Accuracy

Predicted\Real	1	2	3	4	5
1	8202	1440	400	815	1
2	989	2088	366	670	0
3	74	77	224	175	0
4	48	45	73	271	0
5	0	0	0	0	1536

Learning Method based on the Rusboost Algorithm

Figure 3. Confusion matrix for predicting the frequency of using the Internet to contact.

We observe that the accuracy of our algorithm for users in classes 1 and 5 are higher. Some users in class 2 are misclassified as class 1 users and given a higher prediction rate requirement. However, the cost of misclassification is small. For users with small samples in classes 3 and 4, the learning method based on the RUSBoost algorithm that we use can model the minority categories better, so that the accuracy has better performance than other learning algorithms.

3.3. Use of Predictions

Inspired by [42], we map the frequency domain f (values 1–5) to the probability domain p, assigning values of 1, 0.8, 0.6, 0.4, and 0.2, respectively. We use p_V to represent the probability of a user having a video service and p_T to represent the probability of a user having a text service. For example, the value of the frequency domain of the user "using Internet to entertain several times a week" is 2, which means the user has a higher probability of having a video service. Thus, this user's p_V is evaluated by 0.8.

We use R_n^{min} to quantify the requirement rate of users. R_V represents the minimum rate requirement of the user's video service, and R_T represents the minimum rate requirement of the user's text service. Then, for user n, the desired rate requirement R_n^{min} can be calculated as

$$R_n^{min} = p_V(n) * R_V + p_T(n) * R_T \tag{15}$$

4. Many-to-Many Two-Side Subchannel User Matching Algorithm for NOMA-CoMP Systems

It can be known from the system model that the rate of the system is determined by the subchannel and power. Taking into account the complexity of allocation, this section first classifies cell users, and then allocates subchannels to users. The many-to-many two-side subchannel user matching algorithm will be implemented through the following steps.

4.1. Initialization

In order to transform Equation (6) into a many-to-many two-side matching problem and use an equivalent channel gain to improve user fairness, BS b with k subchannels broadcasts a reference signal s_r to all users in the cluster with the same transmission power P_r. Users in the cell using the same subchannel have the same power P_r. The BS b containing k subchannels and m users can obtain the channel gain set $\boldsymbol{H}_b$ of all cell users in this way,

$$\boldsymbol{H}_b = \left\{ \widehat{\boldsymbol{H}}_b(1), \widehat{\boldsymbol{H}}_b(2), ..., \widehat{\boldsymbol{H}}_b(m) \right\}, \forall b \in BS \tag{16}$$

where

$$\widehat{\boldsymbol{H}}_b(n) = \left\{ \gamma_b^1(n), \gamma_b^2(n), \dots, \gamma_b^k(n) \right\}, n = 1, \dots, m \tag{17}$$

4.2. User Classification

The users are classified according to the obtained equivalent channel gain set. If $max(\widehat{\boldsymbol{H}}_b(n)) \leq \varepsilon$ (ε is the threshold for dividing edge users), then the edge user set $\mathbf{U}_b^{(e)} = \{n\}$; otherwise, the cell-center user set $\mathbf{U}_b^{(c)} = \{n\}$. We set a reasonable value (ε = 1.5) in the simulation so that the number of CoMP users in the CoMP cluster and the number of non-CoMP users in each cell are nearly equal. At the same time, according to Section 3, it can be seen that the user requirement rate is predictable. Assuming that the BS can obtain user information completely, we obtain the rate requirement set $\boldsymbol{R}_b^{min}$ of users in the edge user set $\mathbf{U}_b^{(e)}$. If $R_b^{min}(n) \leq \xi$ (ξ is the threshold of user rate requirements), then the high-rate requirement edge user set $\mathbf{U}_b^{(hr)} = \{n\}$; otherwise, the low-rate requirement edge user set $\mathbf{U}_b^{(lr)} = \{n\}$. Moreover, the value of ξ we set is 2.5 so that the number of high rate-requirement users and the number of low rate-requirement users in the cell are nearly equal.

4.3. Calculate the Equivalent Rate Set

Because the BS transmits the signal with the same reference power, the channel gain of a user can be represented by an equivalent channel gain as Equation (16). From Equations (1)–(4) and (16), we can obtain a data rate set for each user of different subchannels when the same reference power is allocated as

$$\widehat{\boldsymbol{R}}_b = \left\{ \widehat{\boldsymbol{R}}_b(1), \widehat{\boldsymbol{R}}_b(2), ..., \widehat{\boldsymbol{R}}_b(m) \right\}, \forall b \in B \tag{18}$$

where

$$\widehat{\boldsymbol{R}}_b(n) = \left\{ R_b^1(n), , R_b^2(n,2) ..., R_b^k(n) \right\}, (n = 1, \dots, m) \tag{19}$$

4.4. Problem Formulation

Let us consider the subchannel set $\mathbf{S}_b$ of each cell and the scheduled users set $\mathbf{U}_b$ as two non-cooperative sets. Players in these two sets in each group are selfish and rational; in other words, they only want to maximize their own interest. If the subchannel $\mathsf{S}_{b,k}$ is allocated to the scheduled user $\mathsf{U}_{b,n}$, it is said that $\mathsf{S}_{b,k}$ and $\mathsf{U}_{b,n}$ are matched with each other to form a pair $\mathsf{S}_{b,k}\Theta\mathsf{U}_{b,n}$, where Θ denotes a mapping relationship. Specially, we give the definition of the mapping relationship between joint subchannels and users in a CoMP cell.

Definition 1. *Given BS groups $\mathbf{B} = \{1,\ldots,B\}$, and each group has two non-cooperative sets, the subchannels group $\mathbf{S} = \{1,\ldots,S\}$ and the users group $\mathbf{U} = \{1,\ldots,U\}$. Θ is a many-to-many mapping between subchannels and users:*

$$
\begin{aligned}
&\textbf{\textit{(a)}} \quad \Theta(\mathsf{U}_{b,n}) \subseteq \mathbf{S}_b \\
&\textbf{\textit{(b)}} \quad \Theta\left(\mathsf{S}_b^k\right) \subseteq \mathbf{U}_b \\
&\textbf{\textit{(c)}} \quad \left|\Theta(\mathsf{U}_{b,n})\right| \leq Q_l \\
&\textbf{\textit{(d)}} \quad \left|\Theta\left(\mathsf{S}_b^k\right)\right| \leq Q_u \\
&\textbf{\textit{(e)}} \quad \mathsf{S}_b^k \in \Theta(\mathsf{U}_{b,n}) \Leftrightarrow \mathsf{U}_{b,n} \in \Theta\left(\mathsf{S}_b^k\right)
\end{aligned}
$$

Condition ***(a)*** *states that each user of a CoMP cell b is matched to a subchannel set of the cell b. Condition* ***(b)*** *expresses that each subchannel is matched to a user set in a CoMP cluster. Condition* ***(c)*** *indicates that the maximum size of scheduled subchannels of user n is Q_l. Condition* ***(d)*** *states the fact that the maximum number of joint subchannel multiplexed users is Q_u.*

In order to describe the competition relationship and matching process among all players in the system better, we assume that each player prefers to work with a player in the other set in the same group. We denote the users' preference list set in group b as

$$\mathcal{Z}_{\mathsf{U}_b} = \left\{\mathbf{Z}_{\mathsf{U}_{b,1}},\ldots,\mathbf{Z}_{\mathsf{U}_{b,U}}\right\}, \quad \forall b \in \mathbf{B} \tag{20}$$

and the set of preference list of subchannels in group b as

$$\mathcal{Z}_{\mathsf{S}_b} = \left\{\mathbf{Z}_{\mathsf{S}_b^1},\ldots,\mathbf{Z}_{\mathsf{S}_b^S}\right\}, \quad \forall b \in \mathbf{B} \tag{21}$$

where we can also call $\mathbf{Z}_{\mathsf{U}_{b,n}}$ and $\mathbf{Z}_{\mathsf{S}_b^k}$ the satisfaction sequence of user n and subchannel k in group b, respectively.

Since one subchannel can be shared by at most Q_u users, the preference set for each subchannel for different subsets of users is expressed as

$$\mathcal{L} \succ \widetilde{\mathcal{L}}\left(\mathcal{L} \subseteq \mathbf{U}_b, \widetilde{\mathcal{L}} \subseteq \mathbf{U}_b\right) \Leftrightarrow R_{\mathcal{S}_b^k}(\mathcal{L}) > R_{\mathcal{S}_b^k}(\widetilde{\mathcal{L}}) \tag{22}$$

which states the fact that $\mathcal{S}_b^k$ is more likely to match to users in $\mathcal{L}$, compared with those in $\widetilde{\mathcal{L}}$. In this paper, the user is scheduled by only one subchannel in the same time slot. So each subchannel preference set in each CoMP cell is represented as

$$\mathcal{S}_b^k \succ \mathcal{S}_b^{\tilde{k}} \Leftrightarrow \gamma_{n,b}^k > \gamma_{n,b}^{\tilde{k}} \tag{23}$$

which means that $\mathsf{U}_{b,n}$ prefers the subchannel in $\mathcal{S}_b^k$ to $\mathcal{S}_b^{\tilde{k}}$. Specifically, the algorithm is as Algorithm 1.

Algorithm 1 **User Classification and Preference Ranking Algorithm**

Input: P_r, ω_n, CoMP user division threshold ε, user rate requirement set $\boldsymbol{R}_b^{min}$, rate requirement division threshold ξ
Output: $\mathsf{U}_b^{(c)}$, $\mathsf{U}_b^{(e)}$, $\mathsf{U}_b^{(hr)}$, $\mathsf{U}_b^{(lr)}$, $\mathcal{Z}_{\mathsf{U}_b}$, $\mathcal{Z}_{\mathsf{S}_b}$
The BS b transmits the same signal P_r to each cell user to obtain the user n equivalent channel gain set $\widehat{\boldsymbol{H}}_b(n)$.
if $max(\widehat{\boldsymbol{H}}_b(n)) \leq \varepsilon$ **then**
  $\mathsf{U}_b^{(e)} = \{n\}$
else
  $\mathsf{U}_b^{(c)} = \{n\}$
end if
for each $n \in \mathsf{U}_b^{(e)}$ **do**
  Obtain the rate requirement set $\boldsymbol{R}_b^{min}$ of users in the edge user set $\mathsf{U}_b^{(e)}$
  if $R_b^{min}(n) \leq \xi$ **then**
    $\mathsf{U}_b^{(hr)} = \{n\}$
  else
    $\mathsf{U}_b^{(lr)} = \{n\}$
  end if
end for
Obtain subchannel preference list and user preference list:
(a) Obtain the user equivalent channel gain set $\widehat{\boldsymbol{H}}_b$ in different subchannels;
(b) According to P_r, ω_n, $\widehat{\boldsymbol{H}}_b$, and $\widehat{\boldsymbol{R}}_b = \left\{\widehat{\boldsymbol{R}}_b(1), \widehat{\boldsymbol{R}}_b(2), ..., \widehat{\boldsymbol{R}}_b(m)\right\}$, get $\widehat{\boldsymbol{R}}_b$;
(c) Sort $\mathcal{S}_b^k$ according to $\widehat{\boldsymbol{H}}_b$, and get $\mathcal{Z}_{\mathsf{U}_b}$;
(d) Sort $\mathsf{U}_{b,n}$ according to $\widehat{\boldsymbol{R}}_b$, and get $\mathcal{Z}_{\mathsf{S}_b}$;

4.5. Many-to-Many Subchannel–User Matching Algorithm in NOMA-CoMP Systems

Compared to the traditional many-to-many two-side matching problem, our optimization problem is more complicated. Our model is applied to ultra dense networks in 5G scenarios, where the number of subchannels and users of CoMP cells may be very large. To solve this matching problem, we propose a subchannel–user matching algorithm for NOMA-CoMP systems based on the Gale–Shapley algorithm.

We modify the traditional Gale–Shapley algorithm [43,44] and propose a many-to-many subchannel–user matching algorithm (MSUMA). The specific extensions of the traditional many-to-many two-side matching algorithm are as follows: (1) We distinguish different BSs in the form of groups, and extend the traditional many-to-many two-side matching problem into multiple groups of interrelated non-cooperative subchannel–user many-to-many two-sided matching problems. (2) The subchannel in each group must not only consider matching with the user in this group, but also consider matching with CoMP user in other groups, i.e., the subchannel in each group need match all CoMP users, and the subchannel–user matching of each group will generate an associated CoMP set. (3) Non-CoMP users and low-rate requirement CoMP users only need to send their curriculum vitaes (CVs) to the subchannel with the highest satisfaction in their cell, while high-rate requirement CoMP users not only send their CVs to the subchannel with the highest satisfaction in their cell, but also send their CVs to the subchannels that have the same resource block in all the cells of the CoMP cluster. (4) The subchannels need to determine whether the matched user is a high-rate requirement CoMP user. For a high-rate requirement CoMP user, it is necessary to determine whether joint CoMP cell selects the CoMP user on the same RB. The high-rate requirement CoMP user is scheduled only when the BS of the joint CoMP cell selects the CoMP user on the same RB. Otherwise, this user will not be scheduled on the RB, e.g., step 8.B. Moreover, for a low-rate requirement CoMP user, it is necessary to determine whether only one cell selects this CoMP user, e.g., step 8.C.

The process of the MSUMA is as follows. As a user expects to be matched to subchannels, it chooses subchannels according to its $\mathcal{Z}_{\mathsf{U}_b}$, i.e., we assume that each user sends its CV to subchannels (non-CoMP users and low-rate requirement CoMP users only send CVs to the preferred subchannels in the local cell, and high-rate requirement CoMP users send CVs to its preferred subchannels in each cell in the CoMP cluster). Then, each subchannel in each cell has the right to reject or accept these CVs according to their respective preferences $\mathcal{Z}_{\mathsf{S}_b}$. When all users have submitted their CVs to their preferred subchannels, the current round of mutual selection ends. The specific description of the algorithm is as Algorithm 2.

Algorithm 2 **Many-to-Many Subchannel–User Matching Algorithm**

Input: $\mathbf{U}_b^{(c)}, \mathbf{U}_b^{(e)}, \mathbf{U}_b^{(hr)}, \mathbf{U}_b^{(lr)}, \mathcal{Z}_{\mathsf{U}_b}, \mathcal{Z}_{\mathsf{S}_b}$

Output: $\left\{\mathcal{S}_b^{JT}\right\}, \left\{\mathcal{S}_b^{DPS}\right\}$

1: Construct a set of all subchannels $\{\mathcal{S}_b match\}$ to label the users that $\mathcal{S}_b$ is currently matched to;

2: Each user $\mathsf{U}_{b,n} \in \mathbf{U}_b$ sends his CV to his favourite subchannel in $\mathbf{Z}_{\mathsf{U}_{b,n}}$: $\mathcal{S}_b^k = \arg\max\limits_{k \in \mathcal{Z}_{\mathsf{U}_{b,n}}} \left[\widehat{\mathbf{H}}_{b,n}\right], \forall n \in \mathbf{U}$

3: **if** $|\{\mathcal{S}_b match\}| < Q_u$ **then**

4: $\quad \mathcal{S}_b^k$ keep $\mathsf{U}_{b,n}$'s offer;

5: **else**

6: $\quad \mathcal{S}_b^k$ selects a set of Q_u satisfying $\mathcal{L} \succ \widetilde{\mathcal{L}}\left(\mathcal{L} \subseteq \mathbf{U}_b, \quad \widetilde{\mathcal{L}} \subseteq \mathbf{U}_b\right)$, update $\{\mathcal{S}_b match\}$;

7: **end if**

8: **Determine whether to schedule edge users:**

(A) For $\mathcal{S}_b^k$ selected $\mathsf{U}_{b,n} \in \mathbf{U}_b^{(e)}$, do:

(B) If $\mathsf{U}_{b,n} \in \mathbf{U}_b^{(hr)}$

- (a) If there is another BS which selects $\mathsf{U}_{b,n}$ at the same time
- (b) $\mathcal{S}_b^k$ keeps $\mathsf{U}_{b,n}$;
- (c) else, $\{\mathcal{S}_b match\}$ - $\{n\}$, update $\{\mathcal{S}_b match\}$.

(C) Else if $\mathsf{U}_{b,n} \in \mathbf{U}_b^{(lr)}$

- (a) If there is no other BS which selects $\mathsf{U}_{b,n}$ at the same time
- (b) $\mathcal{S}_b^k$ keeps $\mathsf{U}_{b,n}$;
- (c) else, $\{\mathcal{S}_b match\}$ - $\{n\}$, update $\{\mathcal{S}_b match\}$.

9: **Update subchannel preference list and user preference list:**

(A) $\mathcal{S}_b^k$ removes the selected users from $\mathbf{Z}_{\mathsf{S}_b^k}$, updates $\mathbf{Z}_{\mathsf{S}_b^k}$;

(B) If $\left|\mathcal{S}_b^k\right| = Q_u$, then remove $\mathcal{S}_b^k$ from $\mathbf{Z}_{\mathsf{U}_{b,n}}$, updates $\mathcal{S}_b^k$; else,only remove scheduled users list in $\mathcal{S}_b^k$ from $\mathbf{Z}_{\mathsf{U}_{b,n}}$, updates $\mathcal{S}_b^k$

(C) If $|\{\mathcal{S}_b match\}| = Q_u \times S, \forall b \in \mathbf{B}$ or $|\{\mathcal{S}_b match\}| = U, \forall b \in \mathbf{B}$, go to Step 10; else, go back to Step 2

10: If $\mathsf{U}_{b,n} \in \mathbf{U}_b^{(hr)}$, where $\mathsf{U}_{b,n} \in \mathcal{S}_b^k$, add $\mathcal{S}_b^k$ to $\left\{\mathcal{S}_b^{JT}\right\}$; else if $\mathsf{U}_{b,n} \in \mathbf{U}_b^{(lr)}$, where $\mathsf{U}_{b,n} \in \mathcal{S}_b^k$, add $\mathcal{S}_b^k$ to $\{\mathcal{S}_b^{DPS}\}$;

11: **End of the algorithm**

Through Algorithm 2, we successfully established the connection between the user and the subchannel, and completed the subchannel allocation of the system. In the next section, we will carry out the power allocation of the entire system to further improve our system, including the subchannel power allocation and power allocation between subchannels.

5. Discrete Power Allocation Algorithm Based on Group Search in NOMA-CoMP Systems

In order to achieve the maximum sum rate of high-speed demand users, we need to optimize the user's power allocation variable $p_{k,n}$. Nevertheless, the power allocation value for paired users is continuous. It is impossible to divide them based on the exhaustive search. However, the power is usually set in discrete steps in existing systems. Therefore, we can discretize the total power into the number of L uniform power levels, and each power level can be expressed as $\xi = P_{total}/L$, using $p^l = \xi * l$ to represent the power level, and $l \in (1, 2, \ldots, L)$. After we discretized the power, the original optimization problem could be optimized based on the idea of group search.

5.1. DPS-CoMP Intra-Subchannel Power Allocation

First, let us discuss the power allocation in the DPS-CoMP channel. In the first step, pair users based on the MSUMA algorithm. After pairing, rank the paired users in descending order according to the equivalent channel gain, and get different paired user pairs $\phi_{m,n}$. After pairing users, the BS transmits L different total power levels for subchannel k. For each user in the user pair $\phi_{m,n}$, the power level allocated to them by the BS is $l' = 0 : 1 : l$, $l'' = l' + 1 : 1 : l$, and $l' + l'' \leq l$. Get the maximum throughput of paired users $\phi_{m,n}$ through iteration. Then obtain the maximum throughput of the current power level l for different user pairs $\phi_{m,n}$ by repeating the above steps. The maximum throughput of subchannel k user pairs is selected as the maximum sum rate, denoted by R_k^l. Finally, adjust the power level l on the subchannel k to achieve the maximum sum rate of the system. The specific description of the algorithm is as Algorithm 3.

Algorithm 3 DPS-CoMP Intra-Subchannel Power Allocation Algorithm

Input: the set of DPS-CoMP users $\{\mathcal{S}_b^{DPS}\}$, the power level constraint L, the number of users M on each subchannel = 2,
Output: R_k^l

```
1:  For user pair φ_{m,n}, assume γ_{k,m} > γ_{k,n}
2:  for each power level l on the subchannel k do
3:    for power level l' = 0 : 1 : l of user m; power level l'' = l' + 1 : 1 : l of user n do
4:      if l' + l'' ≤ l then
5:        According to Equation (1), calculate their throughput R_{k,m}^{l'} and R_{k,n}^{l''}
6:        if R_{k,m}^{l'} > R_min and R_{k,n}^{l''} > R_min then
7:          select max {R_{k,m}^{l'} + R_{k,n}^{l''}} as the maximum sum-rate R_k^l achieved by φ_{m,n}
            under the power level l of the subchannel k in this DPS-CoMP subchannel.
8:        end if
9:      end if
10:   end for
11: end for
12: for power level l = 0 : 1 : L do
13:   repeat steps 2–11, get the maximum sum-rate R_k^l of each power level l on subchannel
      k.
14: end for
```

Through Algorithm 3, the maximum sum-rate R_k^l of each power level l on DPS-CoMP subchannels k can be obtained. In the next step, we introduce the power allocation algorithm in the JT-CoMP subchannel.

5.2. JT-CoMP Intra-Subchannel Power Allocation

We continue to discuss the power allocation within the JT-CoMP channel. After pairing, the paired users are sorted in descending order according to the equivalent channel gain. For the same high-rate requirement edge user p, two paired user pairs $\phi_{m,p}$ and $\phi_{n,p}$ are obtained. Then BS sends L different total power levels for subchannels k, k'. For each user in the user pair $\phi_{m,p}$, the power level allocated to them by the base station is determined by $l^\alpha = 0 : 1 : l$, $l^\lambda = l^\alpha + 1 : 1 : l$, and $l^\alpha + l^\lambda \leq l$. In the same way, for each user in $\phi_{n,p}$, the power level allocated to them by the base station is $l^\beta = 0 : 1 : l'$, $l^\mu = l^\beta + 1 : 1 : l'$, and $l^\beta + l^\mu \leq l'$. Obtain the maximum rate of the edge users in the paired user pair group $\Phi_{m,n,p}$ through iteration, and then obtain the maximum rate of the edge user under the current power level l, l' on the subchannel k, k' for different user pair groups $\Phi_{m,n,p}$ by repeating the above steps. Select the maximum rate of the edge user as the maximum rate, denoted by $R_p^{l^\gamma}$. Finally, adjust the power level l, l' on the subchannel k, k' to achieve the maximum sum-rate of the edge users in the JT-CoMP system. The specific description of the algorithm is as Algorithm 4.

Algorithm 4 **JT-CoMP Intra-Subchannel Power Allocation Algorithm**

Input: the set of JT-CoMP users $\left\{\mathcal{S}_b^{JT}\right\}$, the power level constraint L, the number of users M on each subchannel $= 2$,

Output: $R_{\boldsymbol{K}}^{l^\gamma}$

1: For each user pairs $\phi_{m,p}$ and $\phi_{n,p}$, assume $\gamma_{k,m} > \gamma_{k,p}, \gamma_{k',n} > \gamma_{k',p}$
2: **for** each power level l on the subchannel k **do**
3:   **for** each power level l' on the subchannel k' **do**
4:     **for** power level $l^\alpha = 0:1:l$ of user m; power level $l^\beta = 0:1:l'$ of user n ;power level $l^\gamma = l^\lambda + l^\mu$ of user p, where $l^\lambda = l^\alpha + 1:1:l$, $l^\mu = l^\beta + 1:1:l'$ **do**
5:       **if** $l^\alpha + l^\lambda \leq l$ and $l^\beta + l^\mu \leq l'$ **then**
6:         According to Equations (2)–(4), calculate $R_{k,m}^{l^\alpha}$, $R_{k',n}^{l^\beta}$ and $R_p^{l^\gamma}$;
7:         **if** $R_{k,m}^{l^\alpha} \geq R_{min}$ and $R_{k',n}^{l^\beta} \geq R_{min}$ **then**
8:           select max $\left\{R_p^{l^\gamma}\right\}$ as the maximum rate $R_p^{l^\gamma}$ achieved by $\phi_{m,p}$ and $\phi_{n,p}$ under the power level l and l' of the subchannel k and k' in this JT-CoMP subchannel.
9:         **end if**
10:       **end if**
11:     **end for**
12:   **end for**
13: **end for**
14: **for** power level $l = 0:1:L$ **do**
15:   **for** power level $l' = 1:1:L$ **do**
16:     repeat steps 2–13, get fixed l, the maximum high-rate requirement user rate of each power level l' in the JT-CoMP subchannel group $\boldsymbol{K} = \{k, k'\}$.
17:   **end for**
18:   obtain the maximum high-rate requirement user rate $R_{\boldsymbol{K}}^{l^\gamma}$ in the JT-CoMP subchannel group $\boldsymbol{K}$.
19: **end for**

After determining the power of the paired user through Algorithms 3 and 4, the BS will then allocate power among the subchannels in the next step.

5.3. Inter-Subchannel Power Allocation

For different JT-CoMP and DPS-CoMP subchannels, repeat the above steps to obtain the required maximum rate, which is achieved by different paired users (groups) at different power levels. When the sum of power levels on all subchannels is less than the total power sent by the base station, the maximum user sum-rate in the DPS-CoMP cluster and the maximum edge user sum rate in the JT-CoMP clusters can be realized based on the idea of group search,. Prioritize the minimum rate requirement of the center user and the maximum sum-rate of the edge users in the JT-CoMP clusters, then determine the power allocated by the JT-CoMP subchannel. Finally, allocate the remaining total power to the DPS-CoMP channel to obtain the maximum sum-rate in DPS-CoMP clusters, and determine the power level allocated on each subchannel k. The specific description of the algorithm is as Algorithm 5.

Algorithm 5 **Inter-Subchannel Power Allocation Algorithm**

Input: the maximum sum-rate R_k^l of each power level $l \in L$ on subchannel k; the maximum sum-rate of high-rate requirement $R_{\boldsymbol{K}}^{l^\gamma}$ of each power level $l^\gamma \in L$ on the subchannel group $\boldsymbol{K} = \{k, k'\}$; the number of DPS-CoMP subchannels K; the number of JT-CoMP subchannel groups K'; the power level constraint on each subchannel L.

Output: $R_{sum}^{JT-edge}$;R_{sum}^{DPS}

for subchannel $k = 1 : K$ **do**
  peform Algorithm 3, obtain $R_k^{l_1}, R_k^{l_2}, \ldots, R_k^L$
end for
for subchannel group $\boldsymbol{K} = 1 : K'$ **do**
  peform Algorithm 4, obtain $R_{\boldsymbol{K}}^{l_1^\gamma}, R_{\boldsymbol{K}}^{l_2^\gamma}, \ldots, R_{\boldsymbol{K}}^L$
end for
for power level on the DPS-CoMP subchannel $l = 1 : 1 : L$ **do**
  Each DPS-CoMP subchannel selects one power level l to achieve the maximum sum-rate of R_k^l.
  for power level on the JT-CoMP subchannel $l' = 1 : 1 : L$ **do**
    Each DPS-CoMP subchannel selects one power level l' to achieve the maximum sum-rate of $R_{\boldsymbol{K}}^{l^\gamma}$.
  end for
end for
if the sum of the power of all subchannels is less than the total power P_{total}, and the rate of all users meets their QoS requirements **then**
  exhaustively combinate the maximum edge-user sum-rate $R_{k,k'}^{l^\gamma}$ achieved at each power level l^γ on each subchannel k and k'.
end if
select the maximum $R_{sum}^{JT-edge} = \left\{ R_1^{l_1} + R_2^{l_2} +, \ldots, + R_{\boldsymbol{K}}^{l_{K'}} \right\}$ as the JT-CoMP system achieved maximum edge-user sum-rate, and determine the power allocation for JT-CoMP system; $P_{sum}^{JT} = \left\{ P_1^{l_1} + P_2^{l_2} +, \ldots, + P_{\boldsymbol{K}}^{l_{K'}} \right\}$.
if the sum of the power of all DPS-CoMP subchannels is less than the total power $P_{total} - P_{sum}^{JT}$, and the rate of all users meets their QoS requirements **then**
  exhaustively combinate the maximum edge-user sum-rate R_k^l achieved at each power level l on each subchannel k.
end if
select the maximum $R_{sum}^{DPS} = \left\{ R_1^{l_1} + R_2^{l_2} +, \ldots, + R_K^{l_K} \right\}$ as the DPS-CoMP system achieved maximum sum-rate, and dedetermine the power allocation for DPS-CoMP system.

Through Algorithm 5, we can determine the power allocated to each subchannel, and obtain the user pairing and power allocation of the entire system. In the next section, we will further verify our method through simulation.

6. Simulation Results

6.1. Simulation Scenario Setup

In this section, we evaluate the performance of the proposed discrete power allocation algorithm (DPA) based on group search, and compare the performance with the most classic matching theory with the NOMA-CoMP scheme and the MT NOMA-CoMP scheme. In the following simulations, we assume that each user is scheduled by at most one DPS-CoMP subchannel or one JT-CoMP subchannel, and each subchannel can schedule two users at most. The radius of the cell is set to 200 m; assume that all users are randomly distributed in the respective cells. The total bandwidth of each cell is B = 5 M, and the total transmission power of each base station is set to P_r = 30 dBm. Assume that both the user and the base station are single antenna. The definitions of the symbols in main text are shown in Table 1 and the main simulation parameters are shown in Table 2.

Table 1. List of Symbols.

Symbols	Definition
$\boldsymbol{B}$	The set of BSs
$\boldsymbol{M}$	The set of users in each cell
$\boldsymbol{S}$	The set of subchannels
$x_{k,n}$	The channel selection parameter
$\gamma_{k,n}$	The channel power gain for user n in the subchannel k
$\mathsf{U}_{b,n}$	The user n in cell b
S_b^k	The subchannel k of cell b
$\mathbf{U}_b^{(c)}$	The set of cell edge users in a CoMP cluster
$\mathbf{U}_b^{(e)}$	The set of cell center users in cell b
$\mathbf{U}_b^{(hr)}$	The set of high-rate requirement users in cell b
$\mathbf{U}_b^{(lr)}$	The set of low-rate requirement users in cell b
$\boldsymbol{H}_b$	The channel gain set of cell b
$\boldsymbol{R}_b$	The data rate set of cell b
$\widehat{\boldsymbol{H}}_b(n)$	The equivalent channel gain matrix form BS b to user n
$\widehat{\boldsymbol{R}}_b(n)$	The equivalent data rate matrix form BS b to user n
$\mathcal{Z}$	The preference list set
$\mathbf{Z}$	The preference list matrix

Table 2. Simulation Parameter.

Parameters	**Values**
Parameters	Values
Number of cells	2
Cell radius	200 m
Total bandwidth(B)	5 M
Total power(P_{total})	30 dBm
Noise power spectral density	−173 dBm/Hz
CoMP user division threshold ε	1.5
Rate requirement division threshold ξ	2.5
Fading	Block fading channel
Pass loss model	133.6 + 35 lg(d[km])dB
Minimum rate requirement	1 Mbps

6.2. Results Analysis

Figure 4 shows the sum-rate of high-rate requirement users versus the number of users in the cell on the JT-CoMP subchannels. Each cell has 12 subchannels, which can be divided into DPS-CoMP subchannels and JT-CoMP subchannels according to the user pairing algorithm. We find that the sum rate of edge users with high-rate requirements for each cell using the DPA algorithm, MT algorithm, and NOMA-CoMP algorithm increases with the number of users in each cell. The reason is that as the number of users in each cell increases, more high-rate requirement edge users with higher equivalent channel gains will appear, resulting in more subchannels being divided into JT-CoMP subchannels. Therefore, in the JT-CoMP subchannels of the entire cell, the sum-rate of high-rate requirement users will be higher. However, the difference is that the MT algorithm will slowly decline when the number of users increases to a certain extent. In [31], it was assumed that there is no difference between subchannels. The power is allocated to the users first, and then the subchannels are allocated. Each subchannel is sequentially allocated to CoMP users or non-CoMP users. When the number of users exceeds the maximum number of subchannel scheduling in the cell, user competition becomes more intense, which will further reduce user fairness. Edge users with high-rate requirements lose the opportunity to be scheduled by subchannels because the channel gain is not as good as that of the central user. The MSUMA algorithm proposed in this paper assumes that each subchannel is differentiated. Even when the number of users increases to a certain extent, it can well protect the opportunity of edge users to be scheduled by the subchannels and ensure user fairness. This also causes the sum-rate of high-rate requirement edge users in the DPA algorithm we proposed to be better than other algorithms.

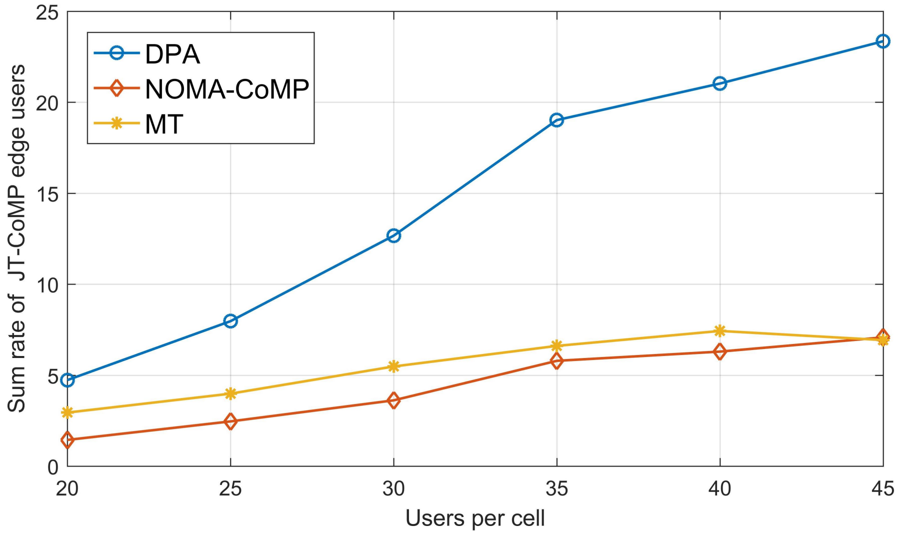

Figure 4. Sum rate of JT-CoMP edge users (Mbps) versus the number of users per cell.

Figure 5 illustrates the relationship between the sum-rate of users and the number of users in the cell on DPS-CoMP subchannels, where each cell has 12 subchannels. It can be seen that as the number of users increases, the sum rate of users on the DPS-CoMP subchannels in each cell using the DPA algorithm, MT algorithm, and NOMA-CoMP algorithm increase with the number of users in each cell. The reason is that there will be more high-rate requirement edge users with higher equivalent channel gains when the number of users in each cell increases, resulting in more subchannels being divided into JT-CoMP subchannels. This also leads to a decrease in the number of DPS-CoMP subchannels, and further leads to a decrease in the user sum-rate of the DPS-CoMP subchannels. We find that the sum rate of the DPS-CoMP subchannels in the DPA algorithm from Figure 5 is greater than that of the traditional NOMA-CoMP algorithm and the MT algorithm. In other words, the DPA algorithm we proposed can serve the edge users with high-speed requirement as much as possible while protecting well the sum rate of the DPS-CoMP system composed of edge users with low-speed requirement.

Figure 6 depicts the sum rate of high-rate requirement users on JT-CoMP subchannels versus the number of cell subchannels, where the number of users in each cell is set to 30. In Figure 6, we can see that when the number of schedulable users in each subchannel is less than the actual number of users, the sum rate of high-rate requirement users in the DPA algorithm, NOMA-CoMP algorithm, and MT algorithm all increase as the number of subchannels increases. Since as the number of subchannels increases, more users can be scheduled by the subchannels, the sum rate will increase. When the actual number of users is less than the maximum number of users that can be scheduled in the subchannel, the rate growth of the three algorithms slows down because all users are scheduled by the subchannel. However, as the number of subchannels increases, users can recommend themselves to subchannels with a better set of preferences to obtain a higher rate.

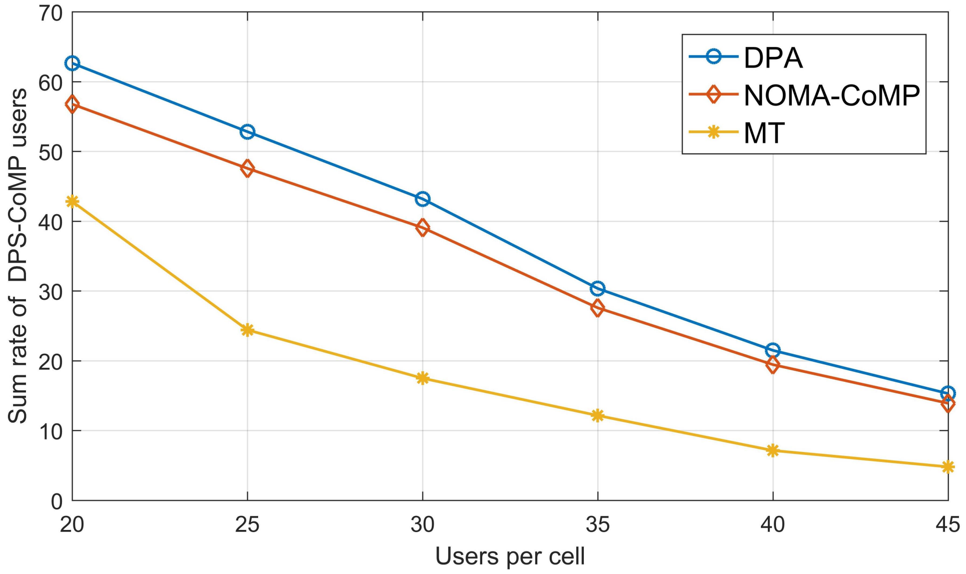

Figure 5. Sum rate of DPS-CoMP users (Mbps) versus the number of users per cell.

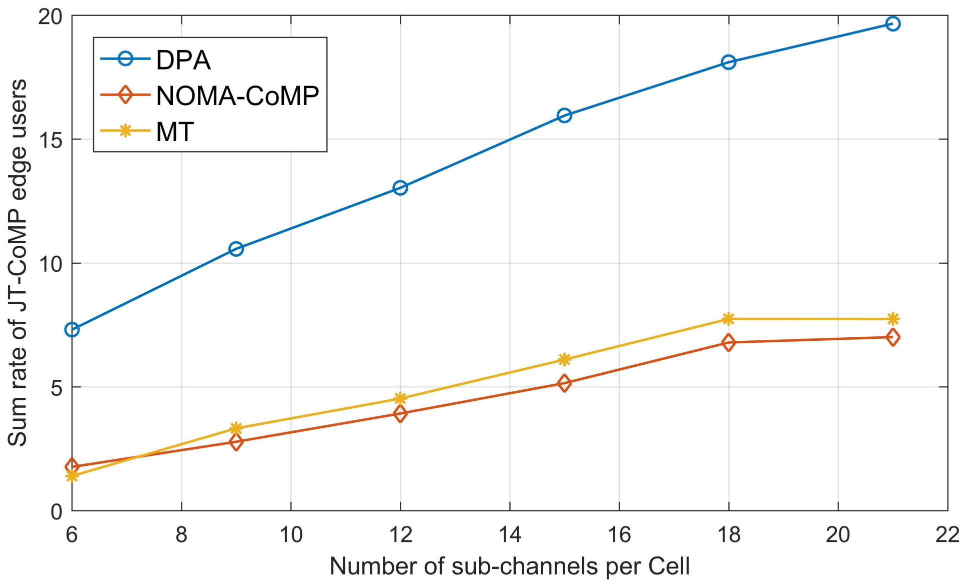

Figure 6. Sum rate of JT-CoMP egde users (Mbps) versus the number of subchannels per cell.

In Figure 7, the performance of user sum rates in DPS-CoMP subchannels and the number of cell subchannels is evaluated. It can be seen from Figure 7 that the user sum rate in the DPS-CoMP subchannel of each cell in the DPA algorithm, the NOMA-CoMP algorithm, and the MT algorithm all increase as the number of subchannels increases. The reason is same as that of the JT-CoMP system. The difference is that when the maximum number of users schedulable in the subchannel is more than the actual number of users in the cell, the sum rate growth rate of users in the DPS-CoMP subchannel does not decrease. In the DPS-CoMP system, our indicator is the sum of the center users' rate and the edge users' rate. At this time, all users will have more choices, and they will be more inclined to send their CVs to subchannels with better channel gain, which will lead to an increase in their own rate, and ultimately lead to an increase in the sum rate of the system.

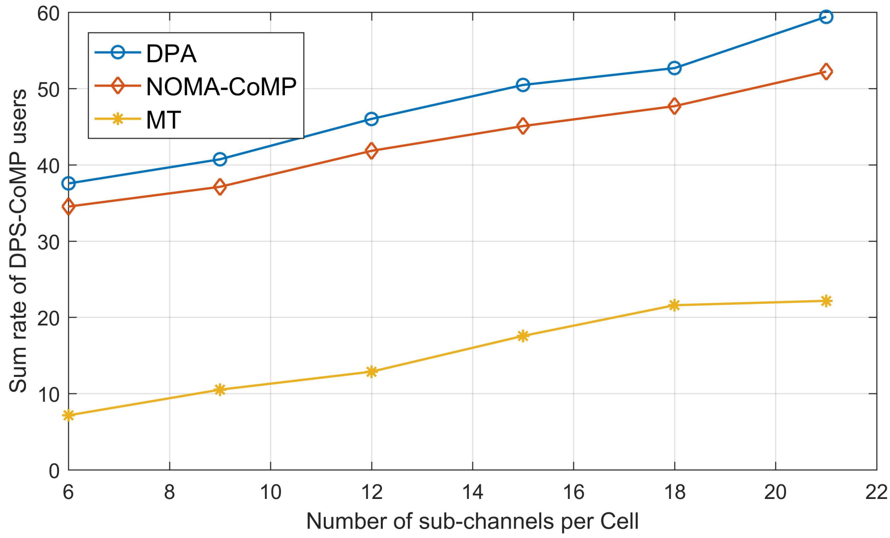

Figure 7. Sum rate of DPS-CoMP users (Mbps) versus the number of subchannels per cell.

7. Conclusions and Future Work

7.1. Conclusions

In this paper, we investigated the problem of multi-cell joint subchannel user pairing and power allocation in the NOMA-CoMP system. While maximizing the sum-rate of edge users with high-rate requirement, we also guarantee the rate of other users and improve the fairness of the system. First, we use deep learning algorithms to predict the users' requirement rate, ensuring that users can be divided into high-rate requirement users and low-rate requirement users. The CoMP cell joint subchannel user pairing problem is transformed into a user pairing algorithm based on two-side many-to-many matching, and the discrete power allocation algorithm based on group search is proposed to allocate the user power of different systems. Simulation results show that the algorithm is superior to the traditional NOMA-CoMP algorithm and the MT-NOMA-CoMP algorithm. It maximizes the rate of edge users with high-rate requirements while the sum rate of our DPS-CoMP users is no lower than other algorithms.

7.2. Future Work

In this paper, corresponding research analysis and algorithm design are carried out for the wireless resource scheduling problem of the NOMA-CoMP system from three perspectives: Rate requirement prediction, user–subchannel pairing and power allocation. However, there are still many problems worthy of further analysis and discussion. In future work, we will investigate making full use of the data related to the user's mobile phone usage habits to improve the accuracy of user demand rate prediction. Moreover, how to use mathematical optimization tools to deduce the optimal solution of the mixed integer nonlinear programming (MINLP) problem of Equation (6) and comparison of the results with the results simulated by the DPA algorithm and the latest related work are worth further study.

Author Contributions: Conceptualization , L.S.; Investigation, L.S.; Methodology, L.S.; Software, L.S.; Validation, L.S.; Writing—original draft, L.S.; Writing—review and editing, J.W. and Y.J. All authors have read and agreed to the published version of the manuscript.

Funding: This research was supported by Science Technology Department of Zhejiang Province grant number 2022C01079 and 2021C01047, and Key Laboratory of Universal Wireless Communications (BUPT), Ministry of Education, China under Grant No. KFKT-2018101.

Data Availability Statement: Not applicable.

Conflicts of Interest: The authors declare no conflict of interest.

References

1. Saito, Y.; Kishiyama, Y.; Benjebbour, A.; Nakamura, T.; Li, A.; Higuchi, K. Non-Orthogonal Multiple Access (NOMA) for Cellular Future Radio Access. In Proceedings of the 2013 IEEE 77th Vehicular Technology Conference (VTC Spring), Dresden, Germany, 2–5 June 2013; pp. 1–5. [CrossRef]
2. Ding, Z.; Fan, P.; Poor, H.V. Impact of User Pairing on 5G Nonorthogonal Multiple-Access Downlink Transmissions. *IEEE Trans. Veh. Technol.* **2016**, *65*, 6010–6023. [CrossRef]
3. Ali, M.S.; Tabassum, H.; Hossain, E. Dynamic User Clustering and Power Allocation for Uplink and Downlink Non-Orthogonal Multiple Access (NOMA) Systems. *IEEE Access* **2016**, *4*, 6325–6343. [CrossRef]
4. Bassoy, S.; Farooq, H.; Imran, M.A.; Imran, A. Coordinated Multi-Point Clustering Schemes: A Survey. *IEEE Commun. Surv. Tutor.* **2017**, *19*, 743–764. [CrossRef]
5. Liu, D.; Han, S.; Yang, C.; Zhang, Q. Semi-dynamic User-Specific Clustering for Downlink Cloud Radio Access Network. *IEEE Trans. Veh. Technol.* **2016**, *65*, 2063–2077. [CrossRef]
6. Lee, D.; Seo, H.; Clerckx, B.; Hardouin, E.; Mazzarese, D.; Nagata, S.; Sayana, K. Coordinated multipoint transmission and reception in LTE-advanced: Deployment scenarios and operational challenges. *IEEE Commun. Mag.* **2012**, *50*, 148–155. [CrossRef]
7. Hayashi, Y.; Kishiyama, Y.; Higuchi, K. Investigations on Power Allocation among Beams in Non-Orthogonal Access with Random Beamforming and Intra-Beam SIC for Cellular MIMO Downlink. In Proceedings of the 2013 IEEE 78th Vehicular Technology Conference (VTC Fall), Las Vegas, NV, USA, 2–5 September 2013; pp. 1–5. [CrossRef]
8. Kimy, B.; Lim, S.; Kim, H.; Suh, S.; Kwun, J.; Choi, S.; Lee, C.; Lee, S.; Hong, D. Non-orthogonal Multiple Access in a Downlink Multiuser Beamforming System. In Proceedings of the MILCOM 2013—2013 IEEE Military Communications Conference, San Diego, CA, USA, 18–20 November 2013; pp. 1278–1283. [CrossRef]
9. Endo, Y.; Kishiyama, Y.; Higuchi, K. A Study on Transmission Power Control Considering Inter-Cell Interference for Non-orthogonal Access with MMSE-SIC in Cellular Uplink. *IEICE Tech. Rep.* **2012**, *112*, 19–24.
10. Ding, Z.; Yang, Z.; Fan, P.; Poor, H.V. On the Performance of Non-Orthogonal Multiple Access in 5G Systems with Randomly Deployed Users. *IEEE Signal Process. Lett.* **2014**, *21*, 1501–1505. [CrossRef]
11. Xu, L.; Zhou, Y.; Wang, P.; Liu, W. Max-Min Resource Allocation for Video Transmission in NOMA-Based Cognitive Wireless Networks. *IEEE Trans. Commun.* **2018**, *66*, 5804–5813. [CrossRef]
12. Xu, L.; Nallanathan, A.; Pan, X.; Yang, J.; Liao, W. Security-Aware Resource Allocation With Delay Constraint for NOMA-Based Cognitive Radio Network. *IEEE Trans. Inf. Forensics Secur.* **2018**, *13*, 366–376. [CrossRef]
13. Di, B.; Bayat, S.; Song, L.; Li, Y. Radio Resource Allocation for Downlink Non-Orthogonal Multiple Access (NOMA) Networks Using Matching Theory. In Proceedings of the 2015 IEEE Global Communications Conference (GLOBECOM), San Diego, CA, USA, 6–10 December 2015; pp. 1–6. [CrossRef]
14. Di, B.; Song, L.; Li, Y. Subchannel Assignment, Power Allocation, and User Scheduling for Non-Orthogonal Multiple Access Networks. *IEEE Trans. Wirel. Commun.* **2016**, *15*, 7686–7698. [CrossRef]
15. Choi, J. Power Allocation for Max-Sum Rate and Max-Min Rate Proportional Fairness in NOMA. *IEEE Commun. Lett.* **2016**, *20*, 2055–2058. [CrossRef]
16. Sawahashi, M.; Kishiyama, Y.; Morimoto, A.; Nishikawa, D.; Tanno, M. Coordinated multipoint transmission/reception techniques for LTE-advanced [Coordinated and Distributed MIMO]. *IEEE Wirel. Commun.* **2010**, *17*, 26–34. WC.2010.5490976. [CrossRef]
17. Li, Q.; Hu, R.Q.; Qian, Y.; Wu, G. Cooperative communications for wireless networks: Techniques and applications in LTE-advanced systems. *IEEE Wirel. Commun.* **2012**, *19*, 22–29. [CrossRef]
18. Tian, Y.; Lu, S.; Nix, A.; Beach, M. A Novel Opportunistic NOMA in Downlink Coordinated Multi-Point Networks. In Proceedings of the 2015 IEEE 82nd Vehicular Technology Conference (VTC2015-Fall), Boston, MA, USA, 6–9 September 2015; pp. 1–5. [CrossRef]
19. Tian, Y.; Nix, A.R.; Beach, M. On the Performance of Opportunistic NOMA in Downlink CoMP Networks. *IEEE Commun. Lett.* **2016**, *20*, 998–1001. [CrossRef]
20. Tian, Y.; Nix, A.; Beach, M. On the Performance of a Multi-Tier NOMA Strategy in Coordinated Multi-Point Networks. *IEEE Commun. Lett.* **2017**, *21*, 2448–2451. [CrossRef]
21. Yang, J.Y.; Huang, W.J. Joint Beamforming and Power Allocation Design in Non-Orthogonal Multiple Access Systems. In Proceedings of the 2016 International Computer Symposium (ICS), Chiayi, Taiwan, 15–17 December 2016; pp. 706–709. [CrossRef]
22. Sun, X.; Yang, N.; Yan, S.; Ding, Z.; Ng, D.W.K.; Shen, C.; Zhong, Z. Joint Beamforming and Power Allocation in Downlink NOMA Multiuser MIMO Networks. *IEEE Trans. Wirel. Commun.* **2018**, *17*, 5367–5381. [CrossRef]
23. Ali, M.S.; Hossain, E.; Kim, D.I. Coordinated Multipoint Transmission in Downlink Multi-Cell NOMA Systems: Models and Spectral Efficiency Performance. *IEEE Wirel. Commun.* **2018**, *25*, 24–31. [CrossRef]
24. Ali, M.S.; Hossain, E.; Al-Dweik, A.; Kim, D.I. Downlink Power Allocation for CoMP-NOMA in Multi-Cell Networks. *IEEE Trans. Commun.* **2018**, *66*, 3982–3998. [CrossRef]
25. Liu, Z.; Kang, G.; Lei, L.; Zhang, N.; Zhang, S. Power Allocation for Energy Efficiency Maximization in Downlink CoMP Systems with NOMA. In Proceedings of the 2017 IEEE Wireless Communications and Networking Conference (WCNC), San Francisco, CA, USA, 19–22 March 2017; pp. 1–6. [CrossRef]
26. Hedayati, M.; Kim, I.M. CoMP-NOMA in the SWIPT Networks. *IEEE Trans. Wirel. Commun.* **2020**, *19*, 4549–4562. [CrossRef]

27. Mirbolouk, S.; Valizadeh, M.; Chehel Amirani, M.; Ali, S. Relay Selection and Power Allocation for Energy Efficiency Maximization in Hybrid Satellite-UAV Networks with CoMP-NOMA Transmission. *IEEE Trans. Veh. Technol.* **2022**, 1. doi: 10.1109/TVT.2022.3152048. [CrossRef]
28. Rezvani, S.; Yamchi, N.M.; Javan, M.R.; Jorswieck, E.A. Resource Allocation in Virtualized CoMP-NOMA HetNets: Multi-Connectivity for Joint Transmission. *IEEE Trans. Commun.* **2021**, *69*, 4172–4185. [CrossRef]
29. Elhattab, M.; Arfaoui, M.A.; Assi, C. Joint Clustering and Power Allocation in Coordinated Multipoint Assisted C-NOMA Cellular Networks. *IEEE Trans. Commun.* **2022**, 1. [CrossRef]
30. Zeng, H.; Zhu, X.; Jiang, Y.; Wei, Z.; Wang, T. A Green Coordinated Multi-Cell NOMA System With Fuzzy Logic Based Multi-Criterion User Mode Selection and Resource Allocation. *IEEE J. Sel. Top. Signal Process.* **2019**, *13*, 480–495. [CrossRef]
31. Singh, R. Sub-channel assignment and resource scheduling for non-orthogonal multiple access (NOMA) in downlink coordinated multi-point systems. In Proceedings of the 2017 20th Conference on Innovations in Clouds, Internet and Networks (ICIN), Paris, France, 7–9 March 2017; pp. 17–22. [CrossRef]
32. Dai, Y.; Liu, J.; Sheng, M.; Cheng, N.; Shen, X. Joint Optimization of BS Clustering and Power Control for NOMA-Enabled CoMP Transmission in Dense Cellular Networks. *IEEE Trans. Veh. Technol.* **2021**, *70*, 1924–1937. [CrossRef]
33. Brueck, S.; Zhao, L.; Giese, J.; Amin, M.A. Centralized scheduling for joint transmission coordinated multi-point in LTE-Advanced. In Proceedings of the 2010 International ITG Workshop on Smart Antennas (WSA), Bremen, Germany, 23–24 February 2010; pp. 177–184. [CrossRef]
34. Feng, M.; She, X.; Chen, L.; Kishiyama, Y. Enhanced Dynamic Cell Selection with Muting Scheme for DL CoMP in LTE-A. In Proceedings of the 2010 IEEE 71st Vehicular Technology Conference, Taipei, Taiwan, 16–19 May 2010; pp. 1–5. [CrossRef]
35. Ohwatari, Y.; Miki, N.; Abe, T.; Nagata, S.; Okumura, Y. Investigation on improvement in channel estimation accuracy using data signal muting in downlink coordinated multiple-point transmission and reception in LTE-Advanced. In Proceedings of the 2011 IEEE Wireless Communications and Networking Conference, Cancun, Mexico, 28–31 March 2011; pp. 1288–1293. [CrossRef]
36. Kojima, K.; Shimbo, Y.; Suganuma, H.; Maehara, F. Deep Learning Based CoMP Transmission Method Using Vehicle Position Information for Taxi Radio Systems. In Proceedings of the 2020 International Conference on Artificial Intelligence in Information and Communication (ICAIIC), Fukuoka, Japan, 19–21 February 2020; pp. 253–256. [CrossRef]
37. Wang, L.; Peters, G.; Liang, Y.C.; Hanzo, L. Intelligent User-Centric Networks: Learning-Based Downlink CoMP Region Breathing. *IEEE Trans. Veh. Technol.* **2020**, *69*, 5583–5597. [CrossRef]
38. Karmakar, R.; Chattopadhyay, S.; Chakraborty, S. A learning-based dynamic clustering for coordinated multi-point (CoMP) operation with carrier aggregation in LTE-advanced. In Proceedings of the 2018 10th International Conference on Communication Systems Networks (COMSNETS), Bangalore, India, 3–7 January 2018; pp. 283–290. [CrossRef]
39. Ahn, J.; Jeon, S.H.; Park, H.S. A Novel Proactive Caching Strategy With Community-Aware Learning in CoMP-Enabled Small-Cell Networks. *IEEE Commun. Lett.* **2018**, *22*, 1918–1921. [CrossRef]
40. Lin, P.; Song, Q.; Song, J.; Jamalipour, A.; Yu, F.R. Cooperative Caching and Transmission in CoMP-Integrated Cellular Networks Using Reinforcement Learning. *IEEE Trans. Veh. Technol.* **2020**, *69*, 5508–5520. [CrossRef]
41. Capdevielle, V.; Monogioudis, P.; Weaver, C.; Pugeat, J.M.; Myers, S. Learning based spectral clustering for LTE downlink CoMP systems. In Proceedings of the 2017 14th IEEE Annual Consumer Communications Networking Conference (CCNC), Las Vegas, NV, USA, 8–11 January 2017; pp. 791–795. [CrossRef]
42. Zheng, Z.; Chi, Q.; Wu, C.; Zhou, W.; Song, L. Human Behavior Based Learning Framework for Spectrum Allocation in Downlink CoMP for 5G Networks. In Proceedings of the 2018 24th Asia-Pacific Conference on Communications (APCC), Ningbo, China, 12–14 November 2018; pp. 173–178. [CrossRef]
43. Roth, A.E.; Sotomayor, M. Two-sided matching, a study in game-theoretic modeling and analysis. *Handb. Game Theory Econ. Appl.* **1992**, *1*, 485–541.
44. Echenique, F.; Oviedo, J. Core many-to-one matchings by fixed-point methods. *J. Econ. Theory* **2004**, *115*, 358–376. [CrossRef]